Journal of Neuropathology and Experimental Neurology
Copyright © 1999 by the American Association of Neuropathologists
Vol. 58, No. 3
March, 1999
pp. 275–287

Quantitative Decrease in Synaptophysin Message Expression and Increase in Cathepsin D Message Expression in Alzheimer Disease Neurons Containing Neurofibrillary Tangles

LINDA M. CALLAHAN, PHD, WILLIAM A. VAULES, MD, AND PAUL D. COLEMAN, PHD

Abstract. Combining immunocytochemistry with in situ hybridization of Alzheimer disease (AD) hippocampus demonstrated a 50% reduction in grain density for synaptophysin message over CA1 pyramidal neurons containing neurofibrillary tangles (NFT) relative to near neighbor NFT-free neurons. This decrease was not global, but was selective since message grain density for the lysosomal protein, cathepsin D, increased 33% in these neurons (relative to NFT-free neurons). Poly A+ message grain density decreased by 25% in NFT neurons. Percent of the cell body containing NFT correlated −0.35 ($p < 0.0001$) with grain density for synaptophysin message. These data verify the concept of altered profiles of gene expression as a function of disease state within single cells and suggest that events associated with NFT formation may lead to altered expression of synaptic messages.

Key Words: CA1; Cathepsin D; Message; NFT; NFT-free; Synaptophysin; Quantitation.

INTRODUCTION

When Alois Alzheimer published the original description of Alzheimer disease (AD) in 1907, he described 2 abnormalities in the brain of his patient: extracellular senile plaques (SP) and intracellular neurofibrillary tangles (NFT) ([1]; for English translation see [2]). Since then numerous additional pathologies have been described in the AD brain (e.g. 3–9). Yet the way(s) in which these pathologies interrelate to form the pathological cascade from first cause of the disease to dementia remains unknown. Indeed, we do not even know which pathologies are central in causing the dementia of AD and which are secondary responses to the degenerative effects of the disease.

Current evidence indicates that the best correlate with the degree of dementia in AD may be decreased synaptic density. Ultrastructural quantitation of synaptic junction density in layer III of area 9 (superior frontal gyrus) in biopsy AD tissue revealed a correlation of $r = 0.77$ ($p < 0.01$) between decreased synaptic density and Mini-Mental State Examination (MMSE) score (10). Additional ultrastructural studies examining biopsy AD tissue (11, 12) and postmortem AD tissue (13, 14) confirmed decreased synaptic junction density in AD. Terry et al (15) established a correlation of 0.73 ($p < 0.01$) between synaptophysin immunoreactivity (IR) in the middle frontal gyrus and MMSE scores in well-fixed AD postmortem tissue. Thus, it has been established both ultrastructurally and immunocytochemically that synaptic density decreases in AD, and that the decrease is significantly correlated with increased dementia. Because the synapse is central to neuronal function, identifying the pathological cascades that lead to decreased synaptic density in AD is critically important to understanding the mechanism(s) by which AD leads to dementia.

Any light- or electron-microscopic examination of diseased regions of AD brain processed to visualize NFT reveals neurons containing NFT immediately adjacent to neurons that are free of NFT. We suggest that the disruptions of cytoskeletal structure and function that are presumed to accompany the formation of NFTs (16), and the consequent disruption of the microtubule transport network of NFT-bearing neurons makes NFT prime suspects for playing a significant role in altered expression of synapse-related messages in AD which may be through a variety of potential mechanisms (e.g. 17–21). Previously, we reported a decrease in mRNA grain density for the synapse-related protein, GAP-43, in NFT neurons compared with near neighbor NFT-free neurons (22), and qualitative observations of a decrease in grain density for synaptophysin message over NFT neurons (23). In this paper we introduce the concept of profiles of expression as a function of disease. We report quantitative data testing the hypothesis that synaptophysin message is selectively reduced in NFT-containing neurons. The data presented here indicate an altered profile of message expression in NFT containing neurons, with message for synaptophysin decreased, and message for the lysosomal enzyme, cathepsin D, increased.

MATERIALS AND METHODS

Subjects and Clinical Evaluation

Tissue was obtained from the Neuropathology Core of the Rochester Alzheimer Disease Center. Cases were defined as AD or control on the basis of clinical (24) and neuropathological

From the Department of Neurobiology & Anatomy (LC, PDC), University of Rochester, Rochester, New York, and the Mayo Clinic (WAV), Rochester, Minnesota.

Correspondence to: Linda M. Callahan, PhD, Department of Neurobiology and Anatomy, University of Rochester, Rochester, NY 14642.

This work was supported by the following grants: LEAD AG09016, NRSA 5T32 AG00107, R01 AG01121, ADC AG08665, the Lucille P. Markey Charitable Trust, and the American Health Assistance Foundation.

Downloaded from https://academic.oup.com/jnen/article/58/3/275/2609741 by guest on 23 April 2024

TABLE
Control and AD Cases Examined by Combined Immunocytochemistry/In situ Hybridization

AD Cases

AD	CDR	Sex	Disease duration	PMI (yr)	Age (h)
Case 1	5	M	15	10.75	93
Case 2	5	F	9	6.75	76
Case 3	4	M	9	16.5	76
Case 4	4	F	13	12.0	81
Case 5	4	F	12	5.5	95
Case 6	1	F	2	14.75	95
Case 7	5	F	10	4.75	85
Case 8	4	F	6	17.0	66
Case 9	5	F	19	12	87
Case 10	5	F	12	6.15	68
Case 11	2	M	10	6.0	84

Age-matched controls

Control	CDR	Sex	Duration	PMI	Age
Case 1	0	M	0	2.5	75
Case 2	0	M	0	18.5	79
Case 3	0	M	0	10.5	66
Case 4	0	M	0	16.10	89
Case 5	0	M	0	14	86
Case 6	0	M	0	4.0	74

CDR = clinical dementia rating, PMI = postmortem interval.

(25) criteria. All final diagnoses were made in a consensus conference of neurologists, psychiatrists, neuropsychologists, and nurses. Fresh tissue blocks were obtained at autopsy and fixed as described below. The average postmortem interval (PMI) for the AD cases used in this study was 10.5 hours with 5 cases less than 7 hours PMI and an overall range of 4.75 to 17 hours. The average postmortem time for the control cases used in this study was 10.9 hours with a range of 2.5 to 18.5 hours.

Cases Studied

The clinical and postmortem information for each case is presented in the Table. An x in the far right column indicates that the cases were studied for all 3 message types. Cases without an x were studied for synaptophysin message only. 11 AD and 6 control cases were examined for synaptophysin message. 4 AD cases were examined for cathepsin D message and 4 AD cases were examined for poly A+ message. Case numbers have been changed for confidentiality.

Tissue Preparation

Tissue blocks collected fresh at autopsy were fixed for 24 hours in phosphate buffered 4% paraformaldehyde. Blocks were then cryoprotected in 30% sucrose in 0.067 M phosphate buffer and frozen in isopentane precooled to −30°C. 18 μm cryostat sections of temporal lobe containing hippocampus were cut, mounted on double-subbed slides (26), and immunoreacted with a monoclonal antibody to NFTs, followed by in situ hybridization with either a ^{35}S labeled synaptophysin antisense riboprobe, a ^{35}S cathepsin D antisense riboprobe, or a ^{3}H labeled poly-U probe.

Slide Preparation

Sections were mounted in a 2 × 2 array so that an age-matched control and an AD section were directly adjacent to each other along the short width of the slide. This enabled control of emulsion artifacts caused by dipping procedures (27). To further control for the possibility of emulsion unevenness, sets of 4 slides containing each case in each of the 4 possible positions on the slide were prepared. Each slide contained 2 AD sections mounted directly adjacent to their age-matched control sections. The purpose of rotating the sections was to eliminate potential interpretation problems due to possible emulsion artifacts (27).

Immunocytochemistry

Monoclonal antibody (mAb) 69, kindly provided by S-H Yen, has been shown to react to a conformational, phosphorylation-independent epitope within the core (PHF-"insoluble") region of PHF-tau (28, 29). Combined immunocytochemistry of mAb 69 with thioflavin S counterstaining demonstrated that mAb 69 recognized 100% of both intra- and extracellular NFT revealed by thioflavin S (28, 29). Additionally, a number of neurons which did not contain thioflavin S staining showed mAb 69 staining, suggesting mAb 69 sensitivity exceeds that of thioflavin S (28). Preliminary study indicated a 1/20 dilution was optimal for detection of mAb 69 positive neurons in our tissue.

Slides containing cryostat-sectioned tissue were placed on a slide warmer for 15 minutes at 45°C, immediately frozen (−80°C) for at least 24 hours, then the following day, desiccated at least 30 minutes. Slides were washed in large volumes of block buffer containing 0.5% BSA and 0.1% horse serum (HS) for 3 hours, then placed into slide mailers (approximately 13 mls for 5 slides) for primary antibody incubation. Primary antibody incubation was at least 16 hours at 4°C with constant, slow agitation. Immunocytochemistry control slides were processed as above but without addition of the primary antibody. Endogenous peroxidase was purposely not removed from our sections since red blood cells served as valuable indicators of potential artifact between probe or emulsion and ICC reaction product (i.e. chemographic artifacts).

Secondary antibody incubation used biotinylated horse-anti-mouse antibody (Vector, 1/1,000) for 1 hour at room temperature. Slides were thoroughly washed with PBS, then incubated with peroxidase-conjugated streptavidin (Vector, 1/1,000) for 1 hour at room temperature. Following another set of washes in PBS, reaction product was visualized using 50 mM Tris, pH 7.6, 0.075% DAB, 0.015% H_2O_2, and 10 mM imidazole. Slides were thoroughly washed in buffer and held overnight in RNAse-free buffer at 4°C until in situ hybridization. In order to preserve the integrity of the intracellular RNA and to prevent degradation during ICC procedures, the RNAse inhibitor, RNAsin, was added to antibody incubations (10 ul RNAsin for every 100 ul serum) and washes were carried out in autoclaved and filtered solutions where possible. Additionally, slides were placed in 4% paraformaldehyde for 20 minutes immediately prior to the in situ hybridization procedure.

Negative controls for the combined immunocytochemistry/in situ hybridization procedure included a set of slides which were not developed for immunocytochemistry and a set of slides

Downloaded from https://academic.oup.com/jnen/article/58/3/275/2609741 by guest on 23 April 2024

which had no primary antibody applied to the sections. NFT staining in the hippocampal region of AD tissue was used as a positive control for immunoreactivity.

In Situ Riboprobes

The synaptophysin cDNA was prepared in our laboratory by RT-PCR based on the published sequence in GenBank using mRNA extracted by us from human brain. A 948-bp portion of the coding region of synaptophysin was used to make the synaptophysin riboprobe. The cDNA began at nucleotide 1266 (corresponding to the initiator Met) and extended to 2 nucleotides before the end of exon six. The synaptophysin DNA was within a PGEM 3 vector, which enabled transcription of both antisense and sense probes. The synaptophysin riboprobe resulting from the cDNA transcription was hydrolyzed to approximately 200 base pairs, as described below.

The plasmid for cathepsin D was generously provided by Dr. Stuart Kornfeld (30) and included the entire coding region from 53 to 1,290 bp. Both cathepsin D (sense and antisense) riboprobes were hydrolyzed to an average of 200 nucleotides as verified on a 1.4% denaturing agarose gel. The ^{3}H-poly U probe (NEN) for poly A+ message was used at 0.9 uCi per slide as per Angerer and Angerer (31) and Griffin et al (32). The poly U probe was estimated to be approximately 400 nucleotides.

Transcription Characteristics

^{35}S-labelled antisense and sense probes were labeled to a final specific activity of 1×10^{8} cpm/ug (33). This activity was obtained by diluting the ^{35}S-UTP with cold S-UTP (NEN, diluted to 200 uM). Riboprobes were transcribed with the Promega Riboprobe system. Antisense and sense probes were obtained using the appropriate RNA polymerase (T7, T3, or SP6). Transcripts were purified using the RNAid System (Bio 101, La Jolla, California) and then (if necessary) hydrolyzed (33) to yield a probe size of ~200 nucleotides. Approximate sizes of probes were checked by gel electrophoresis on a 1.4% denaturing agarose gel.

In Situ Hybridization Procedure

In situ hybridization was as described in Cox et al (34), Angerer and Angerer (33), and Griffin (35) with modifications for fixed human postmortem tissue. Note that the original experiments deriving conditions for riboprobe in situ hybridization are published in Cox et al (34). Some of the important aspects of our procedure included proteinase K (1 μg/ml) at 37°C for 30 minutes, refixation with 4% paraformaldehyde, glycine and acetylation, chloroform treatment during the prehybridization dehydration, and hybridization in a sealed moist chamber at 56°C overnight (12–14 hours). The posthybridization procedure included at least 5 large volume changes of the initial high salt washes (4× SSC) over a period of 2 hours, RNAse treatment (1ug/ml for 30 minutes at 37°C), a high stringency formamide wash (33) performed for 30 minutes at 68°C for cathepsin D and synaptophysin probes, and processing of slides through increasing stringency washes (over a period of 5 hours) ending with 0.1× SSC at 50°C for 15 minutes. Following posthybridization stringency washes and ethanol drying, slides were dipped in NTB2 emulsion in a humid room (greater than 50% humidity, Rogers [27]) under a red filter. They were then slowly dried and placed in a light tight box at 4°C. Slides were developed, fixed, and counterstained with cresyl violet or hematoxylin and eosin. Visualization of signal and counterstain was with an Olympus BH2 microscope.

Controls for Specificity of Probes for In Situ Hybridization

Negative controls for synaptophysin in situ hybridization used sense strand obtained as described above. In addition, sections of liver were processed alongside sections of brain to serve as a negative control for neuron-specific messages. Negative controls for poly U consisted of competition studies with cold poly U and analysis of skin tissue, parenchymal red blood cells, and extracellular NFT. Other controls for the possible effect of prior or combined processing for immunohistochemistry included 1) processing some slides for in situ hybridization first, followed by immunohistochemistry, 2) in situ hybridization followed by congo red staining, and 3) additional slides processed for in situ hybridization only.

Controls for Potential Emulsion Autoradiography Artifact

Emulsion autoradiography provides sensitive analysis of the message levels for individual neurons within tissue. However, controls must be incorporated for a number of potential artifacts, which are due only to the reaction of the silver grains in the emulsion. The potential artifacts that can occur in emulsion autoradiography are thoroughly discussed in Rogers, 1979 (27). For the present study, the following emulsion autoradiographic controls were used.

Negative Chemography Controls: 1) Slides were processed through all steps of the combined ICC/ISH procedure except the addition of probe. 2) Grains over blood cells within the same sections of the tissue hybridized for antisense as well as sense were carefully analyzed. (This is a valuable control for whether a chemography effect has occurred between ICC reaction product and nonspecific sticking of probe or other emulsion reactions. To have this control available we did not remove endogenous peroxidase during the ICC procedure). 3) Comparison was made between sense probe grain density for NFT and NFT-free neurons within the same 40× field. An example of the chemography checks analyzing sense probe over NFT and NFT-free neurons is shown in Figure 1. For cathepsin D message, no increase in grain density was seen in sense controls between NFT (ICC-reacted) and NFT-free (non–ICC-reacted) neurons within the same microenvironments indicating the increase in grain density in NFT neurons hybridized with antisense to cathepsin D message is not due to a chemographic effect with the emulsion.

Positive Chemography Controls: Partial exposure of the emulsion was performed to determine that an even exposure of grains occurred and that no bleaching occurred during the counterstaining procedures. Partial exposure of the emulsion was accomplished by exposing the emulsion in a dip miser to white light for 30 seconds, then mixing the emulsion and dipping 2 to 3 slides containing immunoreacted (but not hybridized) tissue. Analysis of these slides after development indicated that exposed grains were evenly distributed over both ICC-positive and ICC-negative neurons and that bleaching of grains did not occur during the counterstaining procedure.

Downloaded from https://academic.oup.com/jnen/article/58/3/275/2609741 by guest on 23 April 2024

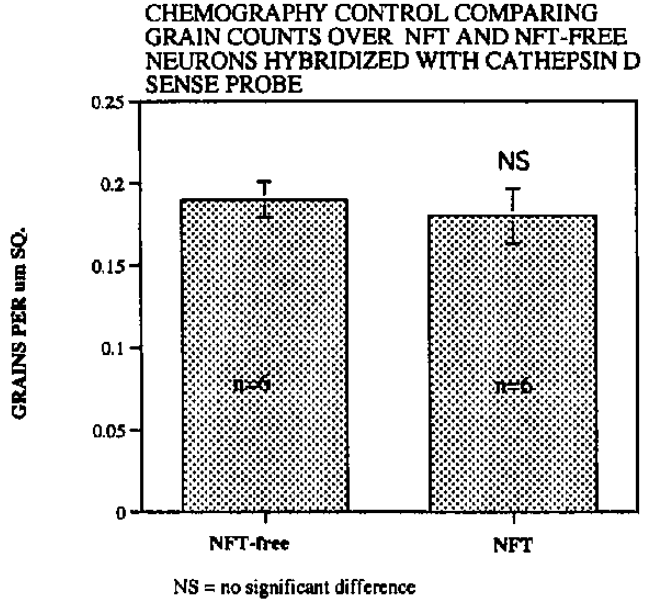

Fig. 1. Chemography control for cathepsin D grain density. *Sense* hybridized neurons were analyzed. No difference in grain density existed between neurons with reaction product for NFT versus neurons without NFT. These data indicate that nonspecific sticking of cathepsin D probe to immunocytochemical reaction product did *not* occur. The data are supported by low grain counts equivalent to background over DAB reacted blood cells in the sections used for analysis of cathepsin D message in NFT neurons. The increase in grain density for cathepsin D message in NFT neurons is therefore a true biological phenomenon of AD neurons.

Stability of mRNA in Postmortem Tissue

A number of studies have indicated that mRNA is relatively stable postmortem (e.g. 36, 37). One laboratory, however, has presented data indicating that each mRNA specie may have unique decay kinetics in postmortem human brain (37). For example, GFAP and alpha-tubulin mRNA were found to have half lives longer than the longest postmortem interval evaluated (13.5 hours), while the half life for low molecular weight neurofilament mRNA was about 6.5 hours, and that of β-actin about 12 hours (37). In a study comparing synaptophysin message levels and postmortem delay, Eastwood et al (38) determined that synaptophysin message did not decrease until 60 hours postmortem. The average postmortem delay for the cases in our study was 10.5 hours for the AD cases and 10.9 hours for the age-matched controls. Additionally, we compared signal for the same message in adjacent NFT and NFT-free neurons within the same microenvironment and postmortem delay of AD and control cases was matched, so control for any postmortem degradation was built in to the experimental design.

Replication of the Results

The synaptophysin message experiments were replicated in quadruplicate and the poly A+ and cathepsin D message experiments were replicated in triplicate. Sections from 11 well characterized AD cases were analyzed for synaptophysin message. Sections from 4 well-characterized AD cases were examined for both cathepsin D and poly A+ messages. Hence, the data reported here are a reproducible phenomenon, not a result of emulsion artifact or of case variation.

Quantitation

Design of the Blind Analysis: Since the neuropathology of AD made it problematic for the observer to be completely blind as to disease state, quantitation of message level over individual neurons was performed as a blind analysis with respect to message type. This was achieved by having a third party thoroughly intermix the slides, affix a coded label to each slide, and carefully record the code next to the original slide number in a log book. To further blind the observer, slides from previous experiments with other messages and antibodies were also covered with coded labels and added to the slides to be quantitated. As a result of this process, the observer was aware that any given slide chosen could have been reacted with one of 5 possible probes and one of 3 different antibodies. Therefore, while the observer counting grains was not necessarily blind with respect to whether a section was from AD or control brain (due to the obvious pathology), or whether a neuron contained immunoreaction product, the probe or antibody used on the sections was unknown.

Criteria for Selection of Neurons: Only neurons with nuclei were analyzed for this study. CA1 of the hippocampal formation was chosen for this analysis since 1) the CA1 zone is a clearly identifiable region, 2) the CA1 zone does not exhibit the neuronal loss with normal aging that has been shown for other regions of the hippocampus (39), and 3) the CA1 zone is a region showing pathological change early in the disease course (40). Key criteria for the neurons included in the study were 1) the neuron must contain a definite nucleus observable at 40× magnification, and 2) a complete neuron needed to be present. Boundaries of a neuron were determined by looking through the microscope and then carefully marking the outlines of the neuron on a video screen. Quantitation began approximately at the end of the "flaring" of the CA3/2 transition zone and the CA1 proper (41). The first neuron encountered containing an obvious nucleus was counted. An equivalent size NFT-free or NFT neuron (depending on the type of the first neuron) within the same 40× field was then counted. If an NFT and a neighbor NFT-free neuron meeting the criteria were not within the original 40× field, an immediately adjacent field was analyzed.

Synaptophysin Message in NFT in Age-matched Control Cases: In age-matched control cases, only a few NFT neurons met our criteria of having clearly visible nuclei. In fact, after decoding the original blind analysis (described above), it was determined that only a few NFT/NFT-free pairs were counted in control sections. To address the interesting question of whether synaptophysin message is reduced in NFT neurons in the absence of clinically demonstrable dementia (i.e. age-matched controls), we performed a separate quantitative study focusing only on control tissue.

To provide the opportunity to study more NFT neurons in controls, the second study required modifying the definition of the CA1 zone to include the area of CA1 closer to the subiculum border. The boundary between CA1 and the subiculum was determined based on the position of the pyramidal layer to the dentate gyrus using a hippocampal atlas as a guide (41).

Downloaded from https://academic.oup.com/jnen/article/58/3/275/2609741 by guest on 23 April 2024

This boundary definition gave us confidence that neurons in the CA1 zone were counted, and that neurons were not counted in the subicular layer (in particular, area subicularis lateralis marginalis [42]). Even with the relaxed definition of the CA1 region, the number of NFT neurons within control CA1 was sparse compared with CA1 regions from patients with clinically apparent dementia. Statistical analysis for these data was as described in the subsequent section "Data and Statistical Analysis."

Accuracy of the Computer Counts: Grain counting was performed using an image analyzer (MicroComputing Imaging Device (MCID), St. Catherines, Ontario, Canada). Neurons were captured by a Videk camera attached to an Olympus BH2 microscope. The image of each neuron was captured into 2 channels: the first channel contained a filtered image of the neuron that enhanced the grains and filtered out the immunocytochemical product, and the second channel contained the unfiltered image.

Prior to quantitative study, considerable time was invested in ensuring the accuracy of computer counts. A study was performed to determine whether grain counts obtained by the MCID computer were as accurate as grain counts obtained manually. The analysis compared the following: 1) the number of grains counted by the computer and the number of grains counted manually for the same neuron using a 100× objective; 2) the number of grains counted manually using a 100× objective and the number of grains manually counted using a 40× objective; 3) the number of grains counted manually using a 40× objective and the number of grains manually counted on the videocaptured image of the same neuron, and 4) the number of grains counted manually using a 40× objective and the number of grains counted by the computer. At least 30 neurons were counted for each of these tests. Correlation coefficients were greater than 0.95 for each of these tests, indicating the computer counted as accurately as would an observer counting grains using a 100× objective.

As a final check of accuracy, grains were counted manually and then compared with the automated computer counts for every twentieth to thirtieth neuron as the actual blind analysis was being performed, yielding a correlation coefficient of 0.99 (Fig. 2).

Three factors were determined to be critical to the accuracy of the grain counts: 1) excellent Kohler illumination of the microscope, 2) low grain density slides, and 3) careful thresholding of the grains over each neuron. Careful attention was paid to quantifying grain density over each neuron by marking the grains using the thresholding feature of the MCID, checking the computer microscope with the marked grains at least twice, then carefully matching the grain marking of the unfiltered image. These 3 steps, combined with the manual counting comparisons taken during the actual blind analysis, ensured confidence in the accuracy of the grain counting by computer. In addition to grain number, measurements including the area of the neuron, the area occupied by NFT within the neuron, and the proportional area of the neuron occupied by grains were obtained by the computer at the same time the grain count for the neuron was obtained. Approximately 700 neurons were quantified for the blind analysis, including neurons for the messages and ICC reaction product reported here. Other neurons were quantified to further blind the analysis for antibody and

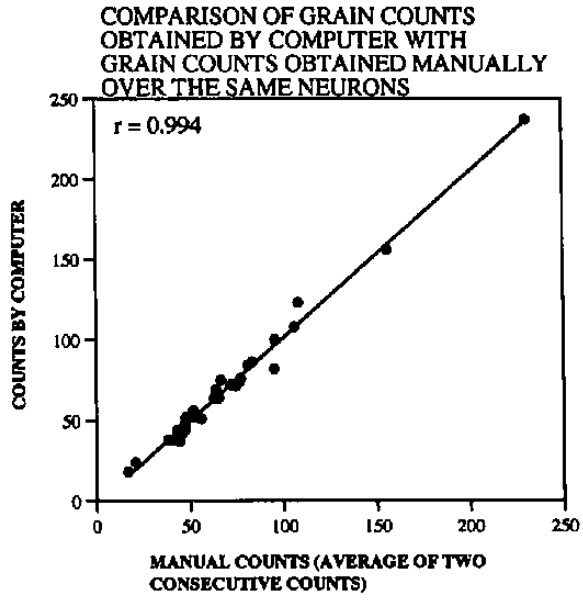

Fig. 2. Correlation of manual grain counts with computer grain counts for 30 neurons counted during the blind analysis. The correlation coefficient for this comparison was r = 0.99, indicating that the computer counts were as accurate as counts obtained manually.

message. Grain counts were expressed as the number of grains per square micron of cell body.

Determination of the Percentage of NFT Within a Neuron: Before determining the grain count for an NFT neuron, a template was made of the area of the neuron. The grain count was then obtained. The neuron was then recaptured and the area template placed over the neuron. The percentage of the neuron occupied by NFT was obtained by marking the area occupied by NFT using the thresholding feature of the MCID.

Data and Statistical Analysis: Following completion of quantitation, the data were exported from the MCID into Microsoft Excel. Slides were decoded and the data regrouped by message type. Data were then matched for adjacent pairs of NFT and NFT-free neurons. Student's *t*-test was performed to analyze differences between NFT and NFT-free populations for each message. A one-way ANOVA and posthoc Scheffe *t*-test (43) were used to analyze ratios of the 3 message types. Correlation of the percentage of NFT occupying the soma with the number of grains over the same neuron was obtained by Cricket Graph III.

RESULTS

Grain Density for Synaptophysin Message Is Reduced in NFT Neurons Compared With Neighboring NFT-Free Neurons in the CA1 Region of Alzheimer Hippocampus

Qualitative observations indicated a reduction of synaptophysin message grain density in NFT neurons relative to NFT-free neurons (Fig. 3a). This decrease appeared to be message species specific since, qualitatively, cathepsin D grain density appeared increased in many

Downloaded from https://academic.oup.com/jnen/article/58/3/275/2609741 by guest on 23 April 2024

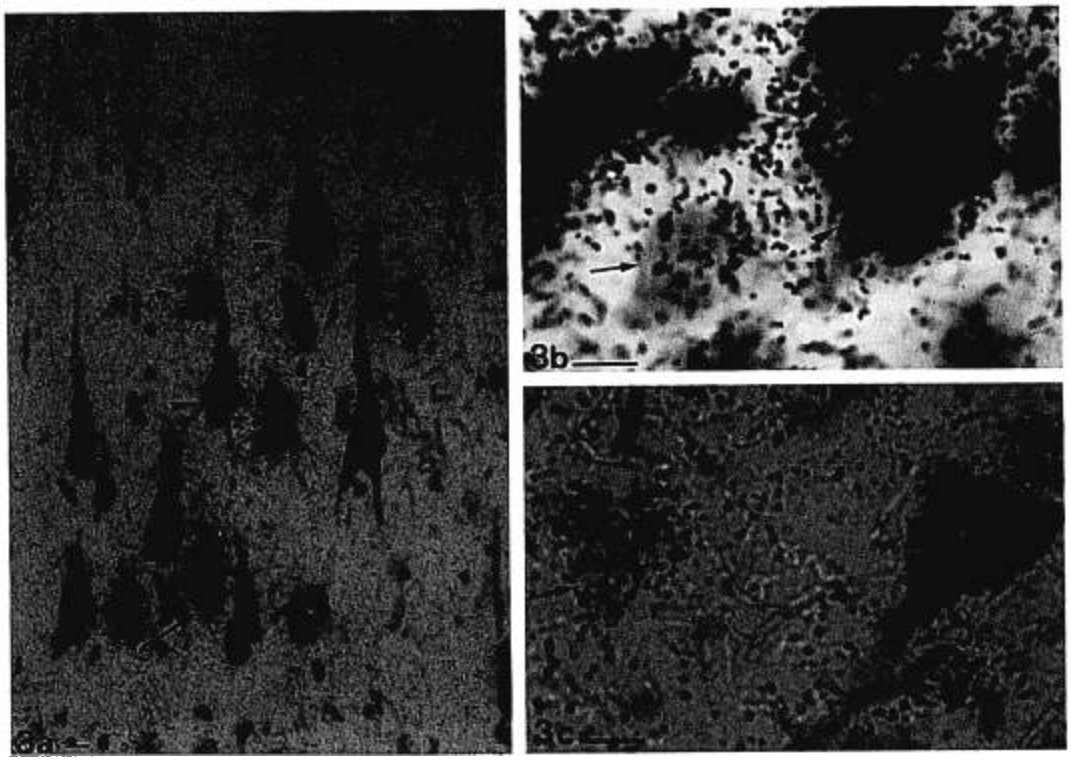

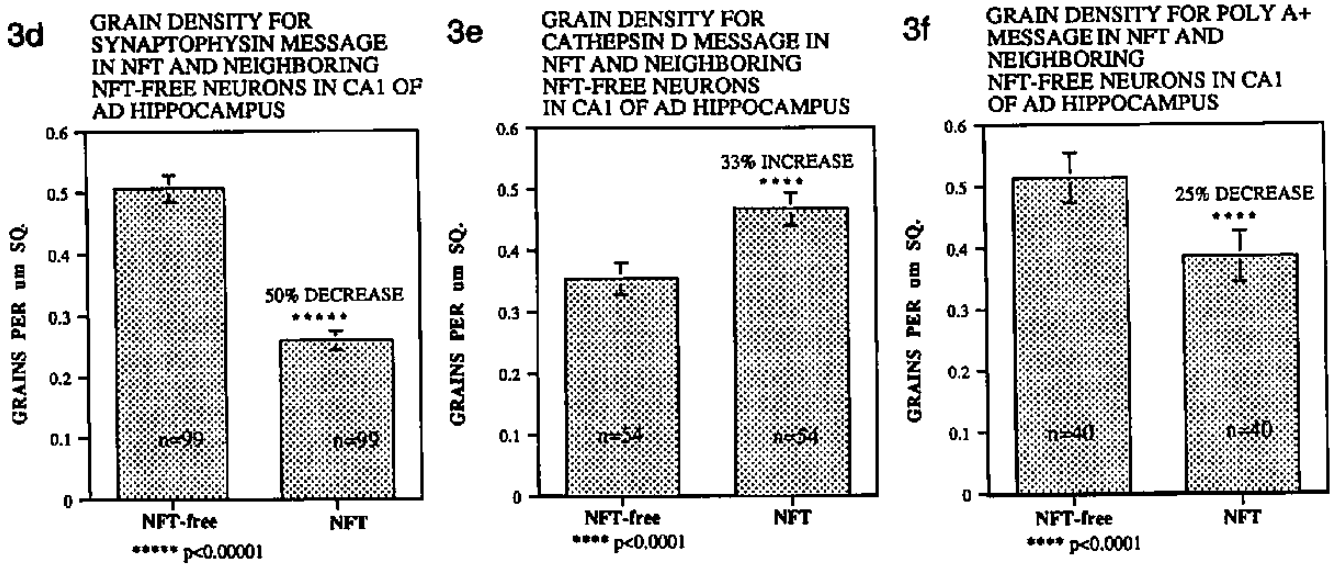

Fig. 3. Combined immunocytochemistry/in situ hybridization for synaptophysin message (a), cathepsin D message (b), and poly A+ message (c) in CA1 of AD hippocampus. Immunocytochemistry was performed with mAb 69 for NFT. Sections were counterstained with cresyl violet. Synaptophysin message grain density decreased 50% over NFT neurons relative to NFT-free neurons (d) ($p < 0.00001$, $t = 8.91$, df = 98). The synaptophysin message reduction in NFT neurons was specific since cathepsin D grain density increased 33% (e) ($p < 0.0001$, $t = 5.36$, df = 53) over NFT neurons compared with neighbor NFT-free neurons. Poly A+ grain density decreased 25% in NFT neurons (f) ($p < 0.0001$, $t = 3.99$, df = 39). These data indicate a specific downregulation of message for one of the most abundant synaptic vesicle proteins in NFT neurons. Bars in a–c = 10 microns. 11 AD cases were quantitated for synaptophysin message, 4 AD for poly A+ message, and 4 AD for cathepsin D message. n values within bars equal the number of neurons examined for each message. Note that slides used for quantitation contained significantly lower grain densities than illustrated in a–c. Figure 3b (cathepsin D qualitative figure) is reprinted from *Neurobiology of Aging* 19, Callahan et al, "Analysis of message expression in single neurons of Alzheimer disease brain," S99–S105, 1998, with permission of Elsevier Science.

Downloaded from https://academic.oup.com/jnen/article/58/3/275/2609741 by guest on 23 April 2024

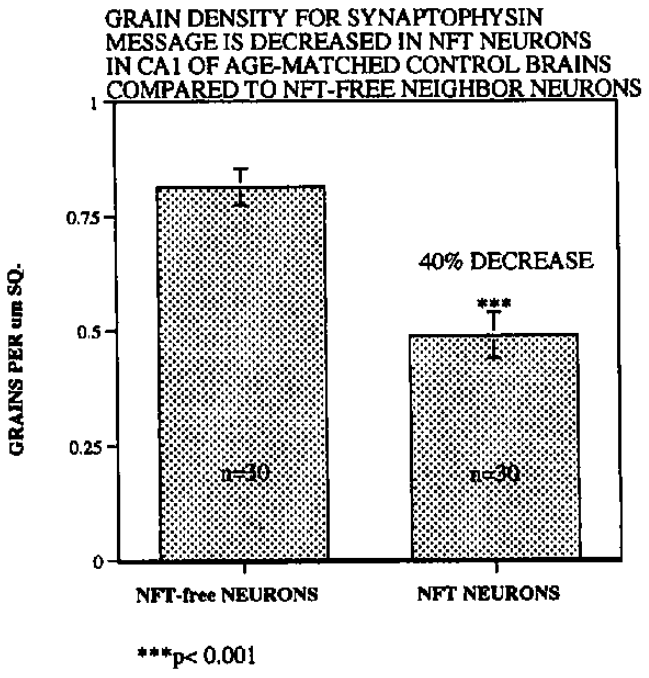

Fig. 4. Grain densities for synaptophysin message over NFT neurons in age-matched control brains compared with neighboring NFT-free neurons. Grain density for synaptophysin message decreased 40% over NFT neurons in controls compared with NFT-free neighbors (Fig. 4) ($p < 0.001$, $t = 5.08$, df = 29). It should be noted that the age-matched controls reported here were Braak stages (I–II), but were clinically nondemented.

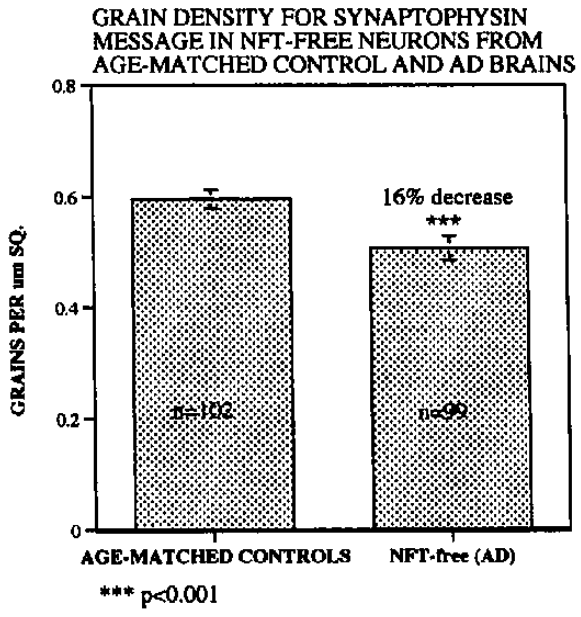

Fig. 5. Grain densities for synaptophysin message in NFT-free neurons in AD and NFT-free neurons in age-matched control brains. NFT-free neurons in AD showed a 16% decrease ($p < 0.001$, $t = 3.21$, df = 98) in grain density for synaptophysin message relative to NFT-free age-matched control neurons indicating that even in end-stage AD, a population of neurons exists which is capable of maintaining near normal levels of synaptophysin message.

NFT neurons (Fig. 3b), and poly A+ message grain density appeared to be only moderately reduced in NFT neurons relative to NFT-free neurons (Fig. 3c).

To determine the actual changes in grain densities, grain counting over NFT and near neighbor NFT-free neuron pairs for synaptophysin message, poly A+ message and cathepsin D message was performed as described above. We assume grain density indicates message level, although not in a one to one proportion. However, it is reasonable to propose a significant reduction in grain density will correspond to a significant reduction in message. Therefore, "message" data in this paper is inferred from the grain counts obtained for that message type.

Grain counts indicated that synaptophysin message was reduced 50% in NFT neurons (Fig. 3d) ($p < 0.00001$, $t = 8.91$, df = 98) relative to neighboring NFT-free neurons. The decrease in synaptophysin message in NFT neurons was selective since grain density for cathepsin D message increased 33% over NFT neurons relative to NFT-free neurons (Fig. 3e) ($p < 0.0001$, $t = 5.36$, df = 53). Grain counts indicated that poly A+ message decreased only 25% in NFT neurons (Fig. 3f) ($p < 0.0001$, $t = 3.99$, df =39).

Synaptophysin Message is Reduced 40% in NFT Neurons in Age-matched Controls Compared With NFT-free Neighbors

A separate study focusing on synaptophysin message in NFT neurons and neighbor NFT-free neurons in age-matched control tissue demonstrated a significant 40% reduction of synaptophysin message in NFT neurons (Fig. 4) ($p < 0.001$, $t = 5.08$, df = 29). It is important to note that the tissue designated as "control" tissue was from patients with no clinically detectable evidence of dementia. However, the Braak stages for all control tissue examined were Braak stage I and II.

A Smaller Decrease in Synaptophysin Message Occurred in NFT-free AD Neurons Relative to NFT-free Age-matched Control Neurons

We consider the NFT-free population of neurons in AD tissue to be at least as important for study as the neuronal population containing NFT. Analysis of NFT-free neurons in AD and age-matched control brains showed that grain density for synaptophysin message in AD NFT-free neurons was reduced by 16% (Fig. 5) ($p < 0.001$, $t = 3.21$, df = 98) compared with NFT-free neurons in age-matched controls.

Downloaded from https://academic.oup.com/jnen/article/58/3/275/2609741 by guest on 23 April 2024

Decreased Grain Density for Synaptophysin Message Correlates Significantly With Increased NFT Burden

Comparison of the number of grains per square micron in NFT neurons and the percentage of NFT occupying the soma of the neuron revealed a significant negative correlation of -0.35 ($p < 0.0001$, Fig. 6a) with $r^2 = 0.12$. These data indicate that as the amount of NFT increases within a neuron, the synaptophysin message decreases. No statistically significant correlation between NFT-burden and grain density was seen for cathepsin D (Fig. 6b) or for poly A+ (Fig. 6c) messages, even though the NFT burden within most neurons was between 25% and 75% for all 3 messages.

Ratios Allow Comparison of Different Message Species Within NFT Neurons

Ratios enable the comparison of all messages on one axis regardless of differences in grain densities arising from technical variations of different autoradiographic experiments (27). Dividing the number of grains/μm^2 over NFT neurons by the number of grains/μm^2 over their neighboring NFT-free neurons yields a ratio of grain densities for each message. A ratio of 1 indicates no difference in grain density between NFT and NFT-free neurons. A ratio of <1 indicates a reduction of grain density over NFT neurons relative to NFT-free neurons, and a ratio of >1 indicates increased grain density over NFT neurons relative to NFT-free neurons. For NFT neurons of CA1 hippocampus in AD, the grain density ratio for cathepsin D message (ratio = 1.48) is increased relative to total message (poly A+) ratio (Fig. 7, $p < 0.01$, ratio = 0.76). In contrast, the grain density ratio for synaptophysin message (ratio = 0.52) is significantly decreased compared with the total message ratio ($p < 0.01$). Thus, overall message content (poly A+) in NFT neurons compared with NFT-free neurons is a poor indicator of the dramatic and selective changes occurring within individual message types in NFT neurons.

DISCUSSION

Message for a Synapse-related Protein is Significantly Reduced in NFT Neurons

The hypothesis being tested by this study is that synaptophysin message is selectively decreased in NFT neurons. Our results demonstrate a 50% reduction ($p < 0.00001$) in grain density for synaptophysin message over AD NFT neurons relative to neighboring NFT-free neurons. Our goal was to examine the relationship between the synaptic marker, synaptophysin, and NFT, an event in the cell body. Although our major concern was with a synaptic marker, we focused on expression of message for this marker at the cell body because of the infeasibility of relating events at a distant synapse to NFT or other events in the cell body of origin. We examined

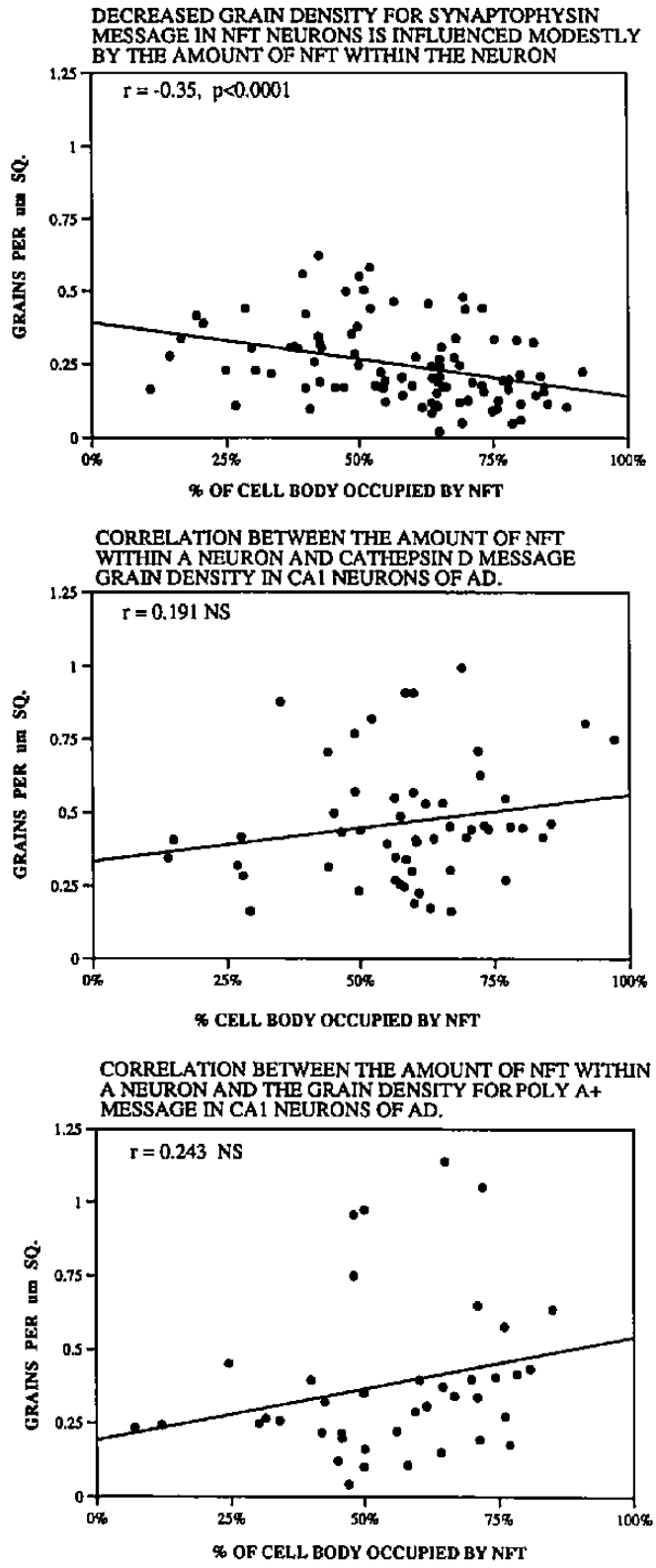

Fig. 6. An inverse correlation exists between grain density for synaptophysin message and the percentage of the cell body occupied by NFT (Fig. 3a) ($r = -0.35$, $p < 0.0001$). Increasing accumulations of NFT had no statistically significant effect on the grain densities for cathepsin D (Fig. 3b) or poly A+ (Fig. 3c) messages.

Downloaded from https://academic.oup.com/jnen/article/58/3/275/2609741 by guest on 23 April 2024

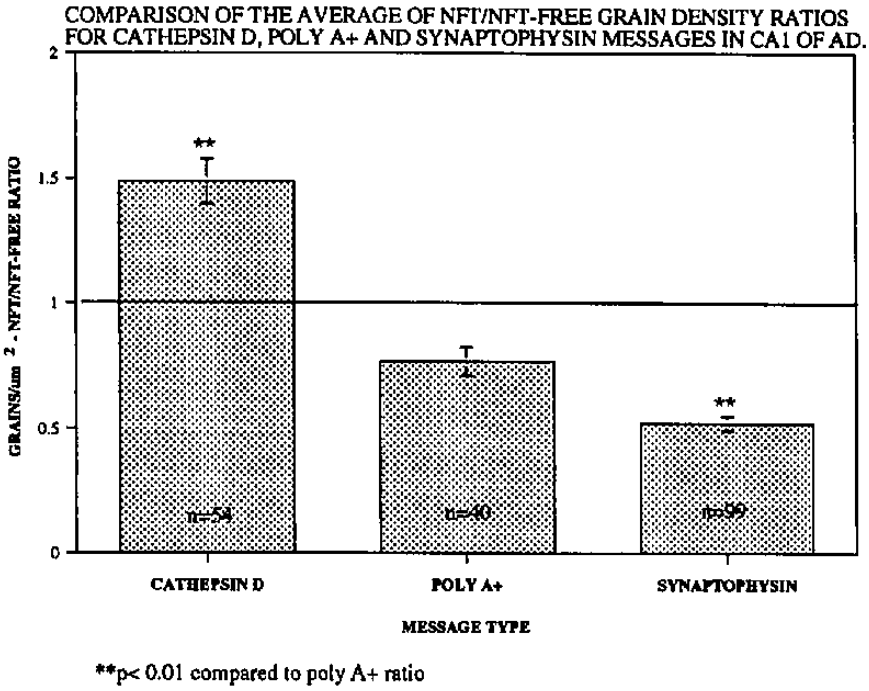

Fig. 7. Ratios permit comparison of all messages on one axis, regardless of differences in grain densities arising from technical variations in different autoradiographic experiments (27). Dividing the number of grains/um² over NFT neurons by the number of grains/um² over their neighboring NFT-free neurons yields a ratio of grain densities for each message. A ratio of 1 indicates no difference in grain density between NFT and NFT-free neurons. A ratio <1 indicates a reduction of grain density over NFT neurons relative to NFT-free neurons, and a ratio >1 indicates increased grain density over NFT neurons relative to NFT-free neurons. For NFT neurons of CA1 hippocampus in AD, the average grain density ratio for cathepsin D message (ratio = 1.48) represents increased expression. By contrast, the average ratio for synaptophysin message (ratio = 0.52) represents a significant decrease of synaptophysin message expression in NFT neurons. The ratio of 0.76 for poly A+ message indicates a modest decrease of total message expression. These data indicate that NFT neurons are actively altering their message expression.

message levels, rather than protein levels, because we wanted to determine overall expression in single postmortem cells and because of the data indicating relative postmortem stability of messages (36, 37). The significance of synaptophysin to cellular function derives, however, from the protein rather than from the message, so it is important to consider the relation between synaptophysin message and protein.

A significant correlation was shown between synaptophysin message and protein levels by Eastwood et al (38) in a study comparing grain counts for synaptophysin message in hippocampal CA1 neurons of nondemented adults with ICC of synaptophysin protein in the regions to which the CA1 neurons project. They reported significant correlations of message in the CA1 region and synaptophysin protein in the subiculum ($p < 0.02$) and deep parahippocampal gyrus ($p < 0.01$). Thus it is reasonable to suggest that synaptophysin message level is proportional to synaptophysin protein level within a neuron, including the projection zone(s) of that neuron, and that a decrease of synaptophysin message in NFT neurons implies a decrease of synaptophysin protein in NFT neurons with consequent synaptic dysfunction.

Supporting the prediction that decreased synaptophysin message correlates to decreased synaptophysin protein, Sze et al (44) recently demonstrated a 55% reduction in synaptophysin protein in membrane fractions from severe AD hippocampus (primarily CA1) using quantitative immunoblotting. A CA1 synaptophysin protein reduction of 55% remarkably complements the 50% synaptophysin message reduction reported here. However, whereas our study focused on comparison of NFT and NFT-free neurons of CA1 pyramidal neurons, Sze et al examined synaptophysin protein content in membranes from unselected CA1 pyramidal neurons, interneurons, and synapses of CA1 afferents (primarily entorhinal cortex layers II and III (perforant path) and CA3/2 pyramidal neurons (the Schaffer collaterals) (41). It is not possible, therefore, to determine the level of reduction of synaptophysin protein occurring in NFT CA1 pyramidal neurons from the Sze et al study. Nonetheless, it is clear that a substantial reduction of synaptophysin protein occurs in CA1 of severe AD. Of even greater interest, Sze et al show hippocampal synaptophysin protein reduction occurs prior to the observation of functional impairments detected by detailed neuropsychological testing in that a 25% reduction of

Downloaded from https://academic.oup.com/jnen/article/58/3/275/2609741 by guest on 23 April 2024

synaptophysin protein level occurred in early (Braak stage defined) AD cases. These data suggest that hippocampal presynaptic defects may be an early, primary change in AD.

Increased Message Levels for Cathepsin D Indicate the Selectivity of Synaptophysin mRNA Reduction in NFT Neurons

Cathepsin D message grain density increased 33% over NFT neurons. This result indicates all message levels in NFT neurons are not decreasing; rather, the cathepsin D data strongly suggest a selective alteration of message expression by NFT neurons. The cathepsin D data also indicate that upregulation of a stress-related message is one response by neurons containing NFT. Our finding of an increase in cathepsin D message in pyramidal neurons of AD CA1 hippocampus is consistent with the increased expression of cathepsin D message and protein in layer III and V pyramidal neurons in AD prefrontal cortex described by Cataldo et al (45). Our data additionally suggest that, at least in hippocampus, an increase in cathepsin D message occurs in NFT neurons relative to adjacent NFT-free neurons. Cataldo et al (45; for review see 46) have proposed that upregulation of cathepsin D message in AD neurons indicates abnormal regulation of the endosomal-lysosomal system and suggest that cathepsin D is involved in abnormal lysosomal processing in AD neurons. Additionally, they proposed upregulation of cathepsin D might be an early event in the pathogenesis of AD.

Poly A+ mRNA is Only Modestly Reduced in NFT Neurons

We report a 25% decrease in grain density for poly A+ message in NFT neurons of CA1 of the hippocampus relative to NFT-free AD neurons. The reduction in grain density for poly A+ message reported here matches the 25% reduction found by Hyman et al (47) in CA1 hippocampus. The 25% decrease in poly A+ message found by us is also well within range of the 33% reduction reported previously by Morrison and Griffin (48) in AD superior frontal gyrus. Hatanpaa et al (49) showed a 20% decrease in AD poly A+ mRNA in middle temporal gyrus NFT neurons containing greater than 50% NFT in the cell body relative to NFT-free neurons. Interestingly, Hatanpaa et al also demonstrated no significant decrease of poly A+ message grain density in NFT neurons containing less than 50% NFT. This is in contrast to our study in which a significant correlation was not seen between the percentage of the cell body filled by NFT and the poly A+ message grain density.

The reduction by about 25% of poly A+ message obviously represents an average of the decreases, increases, and stability of message expression within NFT neurons. Thus the poly A+ message data solidify our belief that analyzing message expression levels of individual proteins in immunocytochemically defined populations of AD tissue will give a clearer understanding of the molecular biology of AD.

Synaptophysin Message is Reduced in CA1 Hippocampal NFT Neurons in Patients Showing no Clinical Evidence of Dementia

The 40% synaptophysin message reduction in age-matched control NFT neurons indicates that dementia severity does not influence synaptophysin message reduction in NFT neurons suggesting that "an NFT neuron is an NFT neuron" regardless of overall disease state. The tissue examined as control tissue was designated as such due to the absence of clinically demonstrable dementia. However, the Braak stages for all control tissue examined were between Braak stage I and II. Additionally, the National Institute on Aging and Reagan Institute Working Group on Diagnostic Criteria for the Neuropathological Assessment of Alzheimer Disease recommended that any pathology, such as the presence of NFT or neuritic plaques, is not normal (50). The presence of such pathologies implies that the individual may be in the early stages of AD despite the lack of clinically demonstrable dementia. Therefore, we consider the "control" population examined in this study to actually represent early AD cases. We emphasize that Braak stage 0 tissue (referred to as "true controls") does not contain NFT within the hippocampus.

The Amount of NFT Within a Neuron Influences the mRNA Level of Synaptophysin, but Not the mRNA Levels of Cathepsin D or Poly A+

A significant negative correlation was obtained between the amount of NFT within a neuron and the grain density for synaptophysin mRNA within that neuron. Significant correlation did not exist for the amount of NFT in a neuron and the grain densities for cathepsin D or poly A+ messages. This suggests that events associated directly or indirectly with NFT formation influence the expression of mRNA for one of the most abundant synaptic vesicle proteins. However, because the r^2 value is only 12%, indicating that only 12% of the variability in synaptophysin message grain density is explained by the amount of NFT within a neuron, other factors besides the actual amount of NFT within the neuron are playing a significant role in the downregulation of synaptophysin message in NFT neurons.

An Emerging Profile of Altered Gene Expression in CA1 NFT Neurons in AD

This discussion will focus on message changes in NFT neurons in the CA1 region, the region of focus for this study. Studies examining message expression levels in AD CA1 NFT neurons compared with NFT-free neurons

Downloaded from https://academic.oup.com/jnen/article/58/3/275/2609741 by guest on 23 April 2024

indicate an emerging expression profile for NFT neurons as follows: cathepsin D mRNA is increased (present study); ERK 2 mRNA (47) and tau mRNA (51) appear to be unchanged; poly A+ mRNA is moderately decreased (47; present study); synaptophysin mRNA (present study), and alpha-tubulin mRNA are significantly reduced (52). A general interpretation of these data is that not all mRNAs in CA1 NFT neurons are reduced. Instead, the expression of individual genes varies in that while message related to synapse function (e.g. synaptophysin) is downregulated, a message related to stress response (cathepsin D) is increased, messages related to the cytoskeleton (tau and tubulin) exhibit variable changes, and one message related to cell signaling pathways (ERKs) may be unchanged. Additionally, two studies (47, present study) have shown that overall mRNA expression (poly A+) in CA1 is a poor indicator of the significant changes occurring in mRNA expression of individual genes within NFT CA1 neurons. These data solidify our conviction that studying individual message profiles in immunocytochemically defined AD neuronal populations will lead to an understanding of specific mRNA expression changes critical to AD pathogenesis.

NFT-free Neurons in AD and Age-matched Control Brains

NFT-free neurons in AD brain show 16% reduction of synaptophysin message relative to NFT-free neurons in control brain. We propose this may be due to 1) reduced synaptophysin message in these neurons may be in those cells that have been shown to accumulate PHF within the processes, but not within the cell body (53, 40), 2) reduced synaptophysin message may be associated with early biochemical events potentially preceding the formation of PHF (i.e. abnormal phosphorylation of tau (for review see 54), or a truncation of tau (55), or jaws and repeat domain abnormalities of tau (for review see (56) and, 3) loss of neurons may lead to a reduction of synaptophysin message in the remaining NFT-free neurons due to decreased activity in the remaining neural net. The above points address factors other than NFT, which may be involved in the reduction of synaptophysin message in NFT neurons. It is essential to address these issues since the r^2 value for correlation of the amount of NFT in a neuron and the grain density for synaptophysin message indicated that only 12% of the reduction of synaptophysin message is accounted for by the amount of NFT within the neuron. This suggests that significant factors, other than the accumulation of NFT, influence the synaptophysin message levels within a neuron. We are currently examining the NFT-free population to determine 1) if decreased synaptophysin message occurs in neurons that contain PHF in the apical dendritic processes but not in the cell bodies, and 2) if altered posttranslational processing of tau is associated with reduction of synaptophysin message.

More Than One Pathway May Lead to Loss of Synaptophysin Message in AD

A number of mechanisms are likely involved in the disruption of synaptophysin message expression in AD. Recent data suggesting neuronal loss in excess of the number of NFT (57) emphasize that an undefined proportion of the overall reduction of synaptophysin message (58) (and protein (38, 44)) loss in AD is probably a consequence of loss of neurons that have not formed NFT. Another path to loss of synaptophysin message, indicated by the present data, could lead to the formation of paired helical filaments (either in the cell body as NFT or in the processes), resulting in an eventual downregulation of synaptophysin message.

Understanding the Mechanism and/or Pathogenesis of AD Through Characterization of Individual AD Neurons

Our data suggest that specific messages are selectively altered at different times in the natural history of disease progression within single neurons. Further study of neurons in AD should permit construction of expression profiles of neurons as disease progresses. Additionally, the data clearly indicate that a number of NFT-free neurons are capable of producing near normal levels of some messages, suggesting some neurons are able to continue to function for many years after the onset of disease. Characterization of individual neurons within the NFT-free population, as well as examination of the neuronal population containing sparse NFT, and neurons containing significant accumulations of NFT should provide a clearer understanding of the molecular pathogenesis of the disease. We propose that careful molecular and immunocytochemical study of individual single cells of AD tissue will yield insights into the pathways leading to loss of synapses through cell dysfunction or death which leads to the cognitive declines of AD.

ACKNOWLEDGMENTS

The authors wish to thank Dr. Lynne Angerer for helpful discussions regarding the in situ hybridization techniques and Dr. Michael Walters for informative discussions regarding the accurate use of the MCID for grain counting. We also thank Ms. Wei Chen and Ms. Janet Cheetham for enthusiastic technical assistance. Drs. Daniel Selski and M. Kerry O'Banion offered numerous insights regarding this study. Mr. George Yannopoulos carefully read this manuscript. The authors are extremely grateful to the Alzheimer and control patients and their families for donation of invaluable tissue. The authors are acutely aware of the sacrifices and arrangements made by the families to participate in these studies. We are also grateful to the Rochester Alzheimer Disease Center members without whose extreme dedication, regardless of substantial disruption to their professional and family lives, the procurement of excellent quality tissue would be impossible. Figure 3b (cathepsin D qualitative figure) is reprinted with permission of Elsevier, publishers of *Neurobiology of Aging*. This work was supported in part by the following grants: LEAD AG09016, 5T32 AG00107, RO1 AG 14441,

Downloaded from https://academic.oup.com/jnen/article/58/3/275/2609741 by guest on 23 April 2024

P30 AG08665, the Lucille P. Markey Charitable Trust, and the American Health Assistance Foundation.

REFERENCES

1. Alzheimer A. Uber eine eigenartige Erkrankung der Hirnrinde. Allg Z Psychiat 1907;64:146–48
2. Alzheimer A, Stelzmann RA, Schnitzlein HN, Murtagh FR. An English translation of Alzheimer's 1907 paper, "Uber eine eigenartige Erkankung der Hirnrinde". Clin Anat 1995;8:429–31
3. Ulrich J. The neuropathology of senile dementia. In: Meier-Ruge W., Karger S. eds. Teaching and training in geriatric medicine, 3. Dementing brain disease in old age. Switzerland, 1993:1–33
4. Koo E, Price DL. The neurobiology of dementia. In: Whitemore P, ed. Contemporary Neurology Series. Philadelphia: F.A. Davis Co., 1993;40:55–91
5. Kosik KS, Qiu WQ, Greenberg S. Cellular signaling pathways and cytoskeletal organization. Ann NY Acad Sci 1996;777:114–20
6. Bissette G, Seidler FJ, Nemeroff CB, Slotkin TA. High affinity choline transporter status in Alzheimer's disease tissue from rapid autopsy. Ann NY Acad Sci 1996;777:197–204
7. Braak H, Braak E. Evolution of the neuropathology of Alzheimer's disease. Acta Neurol Scand 1996;165:3–12
8. Cowburn RF, Fowler CJ, O'Neill C. Neurotransmitters, signal transduction and second-messengers in Alzheimer's disease. Acta Neurol Scand Supp 1996;165:25–32
9. Schmidt ML, Lee VM-Y, Forman M, Chiu T-S, Trojanowski JQ. Monoclonal antibodies to a 100-kd protein reveal abundant a beta-negative plaques throughout gray matter of Alzheimer's disease brains. Am J Pathol 1997;151:69–80
10. DeKosky S, Scheff S. Synapse loss in frontal cortex biopsies in Alzheimer's disease: Correlation with cognitive severity. Ann Neurol 1990;27:457–64
11. Davies C, Mann D, Sumpter P, Yates PA. A quantitative morphometric analysis of the neuronal and synaptic content of the frontal and temporal cortex in patients with Alzheimer's disease. J Neurol Sci 1987;78:151–64
12. Gibson PH. Ultrastructural abnormalities in the cerebral neocortex and hippocampus associated with Alzheimer's disease and aging. Acta Neuropathol 1987;73:86–91
13. Scheff SW, Price DA. Synapse loss in the temporal lobe in Alzheimer's disease. Annals Neurol 1993;33:190–99
14. Scheff SW, DeKosky ST, Price DA. Quantitative assessment of cortical synaptic density in Alzheimer's disease. Neurobiol Aging 1990;11:29–37
15. Terry RD, Masliah E, Salmon DP, et al. Physical basis of cognitive alterations in Alzheimer's disease: Synapse loss is the major correlate of cognitive impairment. Annals Neurol 1991;30:572–80
16. Gray EG, Paula-Barbosa M, Roher A. Alzheimer's disease: Paired helical filaments and cytomembranes. Neuropath Appl Neurobiol 1987;13:91–110
17. Ferreira A, Niclas J, Vale R, Banker G, Kosik KS. Suppression of kinesin expression in cultured hippocampal neurons using antisense oligonucleotides. J Cell Biol 1992;117:595–606
18. Christen B, Bienz M. A cis-element mediating ultrabithorax autoregulation in the central nervous system. Mech Dev 1992;39:73–80
19. Smith K, Sharp Z. A PIT-1 binding site 3′ to the transcription start site inhibits transcription elongation in vitro. Biochem Biophys Res Comm 1991;177:790–96
20. Kim S, Lafyatis R, Kim K et al. Regulation of collagenase gene expression by okadaic acid, an inhibitor of protein phosphatases. Cell Regul 1990;1:269–78
21. Ehrenreich H, Anderson R, Ogino Y et al. Selective autoregulation of endothelins in primary astrocyte cultures: Endothelin receptor-mediated potentiation of endothelin-1 secretion. New Biol 1991;3: 135–41
22. Callahan LM, Selski DJ, Martzen MR, Cheetham JE, Coleman PD. Preliminary evidence: decreased GAP-43 message in tangle-bearing neurons relative to tangle-free neurons in Alzheimer's disease. Neurobiol Aging 1994;15:381–86
23. Callahan LM, Coleman PD. Neurons bearing neurofibrillary tangles are responsible for selected synaptic deficits in Alzheimer's disease. Neurobiol Aging 1995;16:311–14
24. McKhann G, Drachmann D, Folstein K. Clinical diagnosis of Alzheimer's disease: Report of the NINCDS-ADRDA Work Group. Neurology 1984;34:939–44
25. Khachaturian ZS. Diagnosis of Alzheimer's disease. Arch Neurol 1985;42(11):1097–1105
26. Simmons DM, Arriza JL, Swanson LW. A complete protocol for in situ hybridization of messenger RNAs in brain and other tissue with radiolabeled single-stranded RNA probes. J Histotech 1989;12: 169–81
27. Rogers AW. Part I. The bases of autoradiography. New York: Elsevier/North-Holland Biomedical Press, 1979:61–132
28. Yen SH, Crowe A, Dickson DW. Monoclonal antibodies to Alzheimer neurofibrillary tangles. 1. Identification of polypeptides. Amer J Path 1985;120:282–91
29. Yen SH, Dickson DW, Crowe A, Butler M, Shelanski ML. Alzheimer's neurofibrillary tangles contain unique epitopes and epitopes in common with the heat-stable microtubule associated proteins tau and MAP 2. Amer J Path 1987;126:81–91
30. Faust PL, Kornfeld S, Chirgwin JM. Cloning and sequence analysis of cDNA for human cathepsin D. Proc Natl Acad Sci 1985;82: 4910–14
31. Angerer LM, Angerer RC. Detection of poly A+ RNA in sea urchin eggs and embryos by quantitative in situ hybridization. Nuc Acids Res 1981;9:2819–40
32. Griffin WST, Ling C, White CL, Morrison-Bogorad M. Polyadenylated messenger RNA in paired helical filament-immunoreactive neurons in Alzheimer disease. Alz Dis Assoc Dis 1990;4:69–78
33. Angerer RC, Angerer LM. Localization of mRNAs by in situ hybridization. Methods in Cell Biology 1991;35:37–71
34. Cox KH, DeLeon DV, Angerer LM, Angerer RC. Detection of mRNAs in sea urchin embryos by in situ hybridization using asymmetric RNA probes. Dev Biol 1984;101:485–502
35. Griffin WST. Methods for hybridization and quantitation of mRNA in individual brain cells. In: Valentino KL, Eberwine JH, Barchas JD. eds. In situ hybridization. Applications to neurobiology. New York: Oxford University Press, 1987; Chapter 5
36. Johnson S, Morgan D, Finch CE. Extensive post-mortem stability of RNA from rat and human brain. J Neuroscience Res 1986;16: 267–80
37. Lukiw WJ, Wong L, McLachlan DR. Cytoskeletal messenger RNA stability in human neocortex: Studies in normal aging and in Alzheimer's disease. Internat J Neurosci 1990;55:81–88
38. Eastwood SL, Burnet PWJ, McDonald B, Clinton J, Harrison PJ. Synaptophysin gene expression in human brain: A quantitative in situ hybridization and immunocytochemical study. Neurosci 1994;59:881–92
39. West MJ. Regionally specific loss of neurons in the aging human hippocampus. Neurobiol Aging 1993;14:287–93
40. Braak E, Braak H, Mandelkow E. A sequence of cytoskeleton changes related to the formation of neurofibrillary tangles and neuropil threads. Acta Neuropath 1994;87:554–67
41. Amaral DG, Insausti R. Hippocampal Formation PY −1990. In: The human nervous system. New York: Academic Press, 1990: 711–55
42. Braak H. The Hippocampal Formation. In: Barlow, HB, Bizzi, E, Florey, E, Grusser, O-J, van der Loos, H. eds. Architectonics of the human telencephalic cortex, New York: Springer-Verlag, 1980;Chapter 5:26–48

Downloaded from https://academic.oup.com/jnen/article/58/3/275/2609741 by guest on 23 April 2024

43. Sproull N. The Scheffe test for posthoc multiple comparisons after an ANOVA. In: Sproull N. ed. Handbook of research methods. Meeutchen, NJ: The Scarecrow Press, Inc., 1988:277–87
44. Sze CI, Troncoso JC, Kawas C, Mouton P, Price DL, Martin LJ. Loss of the presynaptic vesicle protein synaptophysin in hippocampus correlates with cognitive decline in Alzheimer disease. J Neuropathol Exptl Neurol 1997;56:933–44
45. Cataldo AM, Barnett JL, Berman SA, et al. Gene expression and cellular content of cathepsin D in Alzheimer's disease brain: Evidence for early up-regulation of the endosomal-lysosomal system. Neuron 1995;14(3):671–80
46. Nixon RA, Cataldo AM. The endosomal-lysosomal system of neurons: New roles. Trends in Neurosciences 1995;18:489–96
47. Hyman BT, Elvhage TE, Reiter J. Extracellular signal regulated kinases. Localization of protein and mRNA in the human hippocampal formation in Alzheimer's disease. Am J Path 1994;144:565–72
48. Morrison MR, Griffin WS. The isolation and in vitro translation of undegraded messenger RNAs from human postmortem brain. Analyt Biochem 1981;113:318–24
49. Hatanpaa K, Brady DR, Stoll J, Rapoport SI, Chandrasekaran K. Neuronal activity and early neurofibrillary tangles in Alzheimer's disease. Ann Neurol 1996;40:411–20
50. The National Institute on Aging, and Reagan Institute Working Group on Diagnostic Criteria for the Neuropathological Assessment of Alzheimer's Disease. Consensus recommendations for the postmortem diagnosis of Alzheimer's Disease. Neurobiol Aging 1997;18:S1–S2
51. Kosik KS, Crandall JE, Mufson EJ, Neve RL. Tau in situ hybridization in normal and Alzheimer brain: Localization in the somatodendritic compartment. Ann Neurol 1989;26:352–61
52. Brion JP, Flament-Durand J. Distribution and expression of the alpha-tubulin mRNA in the hippocampus and the temporal cortex in Alzheimer's disease. Path Res Pract 1995;191:490–98
53. Schmidt ML, Murray JM, Trojanowski JQ. Continuity of neuropil threads with tangle-bearing and tangle-free neurons in Alzheimer disease cortex. A confocal laser scanning microscopy study. Mol Chem Neuropath 1993;18:299–312
54. Trojanowski JQ, Lee VMY. Phosphorylation of paired helical filament tau in Alzheimer's disease neurofibrillary lesions: Focusing on phosphatases. FASEB Journal 1995;9:1570–76
55. Wischik CM, Edwards PC, Lai RY, et al. Quantitative analysis of tau protein in paired helical filament preparations: Implications for the role of tau protein phosphorylation in PHF assembly in Alzheimer's disease. Neurobiol Aging 1995;16:409–17
56. Mandelkow EM, Biernat J, Drewes G, Gustke N, Trinczek B, Mandelkow E. Tau domains, phosphorylation, and interactions with microtubules. Neurobiol Aging 1995;16:355–62
57. Gomez-Isla T, Price JL, McKeel DWJ, Morris JC, Growdon JH, Hyman BT. Profound loss of layer II entorhinal cortex neurons occurs in very mild Alzheimer's disease. J Neurosci 1996;16:4491–4500
58. Heffernan JM, Eastwood SL, Nagy Z, Sanders MW, McDonald B, Harrison PJ. Temporal cortex synaptophysin mRNA is reduced in Alzheimer's disease and is negatively correlated with the severity of dementia. Exptl Neurol 1998;150: 235–39

Received June 11, 1998
Revision received October 28, 1998
Accepted December 14, 1998

Downloaded from https://academic.oup.com/jnen/article/58/3/275/2609741 by guest on 23 April 2024